Environment International 68 (2014) 200–208

Contents lists available at ScienceDirect

Environment International

journal homepage: www.elsevier.com/locate/envint

Using the Community Multiscale Air Quality (CMAQ) model to estimate public health impacts of $PM_{2.5}$ from individual power plants

Jonathan J. Buonocore [a,b,*,1], Xinyi Dong [c], John D. Spengler [a,b], Joshua S. Fu [c], Jonathan I. Levy [b,d]

[a] Center for Health and Global Environment, Department of Environmental Health, Harvard School of Public Health, Boston, MA 02215, United States
[b] Department of Environmental Health, Harvard School of Public Health, Boston, MA 02215, United States
[c] Department of Civil and Environmental Engineering, University of Tennessee at Knoxville, Knoxville, TN 37996-2010, United States
[d] Department of Environmental Health, Boston University School of Public Health, Boston, MA 02115, United States

ARTICLE INFO

Article history:
Received 16 October 2013
Accepted 30 March 2014
Available online 23 April 2014

Keywords:
CMAQ
Air quality
Impacts of electrical generation
$PM_{2.5}$
Atmospheric modeling

ABSTRACT

We estimated $PM_{2.5}$-related public health impacts/ton emitted of primary $PM_{2.5}$, SO_2, and NO_x for a set of power plants in the Mid-Atlantic and Lower Great Lakes regions of the United States, selected to include varying emission profiles and broad geographic representation. We then developed a regression model explaining variability in impacts per ton emitted using the population distributions around each plant. We linked outputs from the Community Multiscale Air Quality (CMAQ) model v 4.7.1 with census data and concentration–response functions for $PM_{2.5}$-related mortality, and monetized health estimates using the value-of-statistical-life. The median impacts for the final set of plants were $130,000/ton for primary $PM_{2.5}$ (range: $22,000–230,000), $28,000/ton for SO_2 (range: $19,000–33,000), and $16,000/ton for NOx (range: $7100–26,000). Impacts of NO_x were a median of 34% (range: 20%–75%) from ammonium nitrate and 66% (range: 25%–79%) from ammonium sulfate. The latter pathway is likely from NO_x enhancing atmospheric oxidative capacity and amplifying sulfate formation, and is often excluded. Our regression models explained most of the variation in impact/ton estimates using basic population covariates, and can aid in estimating impacts averted from interventions such as pollution controls, alternative energy installations, or demand-side management.

1. Introduction

Ambient fine particulate matter ($PM_{2.5}$ — particles with aerodynamic diameter ≤2.5 μm) has been linked to higher risks of all-cause, cardiovascular, and lung cancer mortality (National Research Council, 2010; Pope and Dockery, 2006; Pope et al., 2002; Schwartz et al., 2008; Zanobetti and Schwartz, 2009); in 2005, this amounted to between 130,000 and 320,000 excess deaths in the United States (U.S.) (Fann et al., 2012b). A substantial portion of ambient $PM_{2.5}$ in the U.S. is attributable to electricity generation with fossil fuels. In 2005, electricity generation was responsible for 69% of sulfur dioxide (SO_2) and 17% of nitrogen oxide (NO_x) emissions, both of which form $PM_{2.5}$ through secondary atmospheric chemistry, and for 19% of primary $PM_{2.5}$ emissions, and projections indicate that electricity generation will continue to be a substantial contributor to these emissions in upcoming years (Fann et al., 2012a; U.S. Environmental Protection Agency).

Public health impacts of emissions from power plants in the U.S. have been examined recently at a variety of scales, and using different atmospheric chemistry and transport models (Epstein et al., 2011; Fann et al., 2009, 2012a,b, 2013; Levy and Spengler, 2002; Levy et al., 2002, 2003; Machol and Rizk, 2013; Muller and Mendelsohn, 2009; Muller et al., 2011; National Research Council, 2010; U.S. Environmental Protection Agency Office of Air Quality Planning and Standards, 2006; U.S. Environmental Protection Agency Office of Air and Radiation, 2011a,b; U.S. EPA Office of Air Quality Planning and Standards, 2009; Weber et al., 2010). These studies have generally used one of two approaches: 1) reduced-form atmospheric chemistry and transport models to produce impact/ton estimates for a large set of individual power plants; 2) response-surface models (RSM) derived from a series of specifically-designed Community Multiscale Air Quality (CMAQ) model simulations that provide impact/ton estimates for a generalized set of source classes (including fossil-fuel power plants and many other sources) in different regions in the U.S. (Arunachalam et al., 2011; Byun and Schere, 2006; Fann et al., 2009, 2012a,b; Levy et al., 2012; U.S. Environmental Protection Agency Office of Air Quality Planning and Standards, 2006). CMAQ is a well-vetted, peer-reviewed,

Abbreviations: CMAQ model, Community Multiscale Air Quality model; $PM_{2.5}$, particulate matter 2.5 (airborne particulate with aerodynamic equivalent diameter ≤ 2.5 μm); SO_2, sulfur dioxide; NO_x, nitrogen oxides; VSL, value of statistical life; eGRID, Emissions and Generation Resource Integrated Database; NEI, National Emissions Inventory; U.S. EPA, U.S. Environmental Protection Agency; RSM, Response Surface Model.

* Corresponding author at: Center for Health and Global Environment, Department of Environmental Health, Harvard School of Public Health, Boston, MA 02215, United States. Tel.: +1 617 384 8530.
E-mail addresses: jbuonocore@mail.harvard.edu (J.J. Buonocore), xdong1@utk.edu (X. Dong), spengler@hsph.harvard.edu (J.D. Spengler), jsfu@utk.edu (J.S. Fu), jonlevy@bu.edu (J.I. Levy).
[1] Author had affiliation #2 during majority of work.

http://dx.doi.org/10.1016/j.envint.2014.03.031
0160-4120/

comprehensive atmospheric chemistry and transport model that includes complex chemical pathways for secondary $PM_{2.5}$ formation and interactions with background chemistry and other emission sources (Arunachalam et al., 2011; Byun and Schere, 2006; Levy et al., 2012). While CMAQ has many strengths, applying it to estimate impacts individually for a large number of sources would be a time- and resource-intensive process (Fann et al., 2012a,b). Recent innovations using CMAQ, such as the decoupled direct method (DDM), can potentially allow for greater source-specific impact assessment, but such methods remain too computationally intensive to characterize all individual sources within a large geographic domain (Bergin et al., 2008; Itahashi et al., 2012).

Studies using both reduced-form models and CMAQ RSM outputs produced monetized estimates of impact/ton emitted for fossil-fuel power plants, and found that they varied widely among regions and emitted pollutants (Fann et al., 2009; Levy et al., 2009; Muller and Mendelsohn, 2007, 2009; Muller et al., 2011; National Research Council, 2010). This variability is largely due to plant location, which determines both meteorological and geographical conditions and population distributions around the plants (Levy et al., 2009; Muller and Mendelsohn, 2007, 2009; Muller et al., 2011; National Research Council, 2010). The reduced-form models can provide estimates for individual power plants, therefore including variability among plants and within region, but they have simplified meteorology and do not include many complex chemical pathways of secondary $PM_{2.5}$ formation (Greco et al., 2007; Innovative Strategies and Economics Group, Office of Air Quality Planning and Standards, U.S. Environmental Protection Agency, 1999; Levy et al., 2009; U.S. Environmental Protection Agency, 1999). As a result, these models may mischaracterize how emissions affect $PM_{2.5}$ concentrations downwind, especially at long distances from a source. Since a substantial part of the health impact from an emission source can occur beyond 500 km from the source (Levy et al., 2002, 2003), accurately modeling the contribution of emissions to $PM_{2.5}$ concentrations at these distances is critical. Studies to date using RSM provide impact/ton estimates by source class and region that include complex atmospheric chemistry and better characterization of impacts far from the source, but provide estimates based on source region, not an individual source's location (Fann et al., 2009, 2012a,b; U.S. Environmental Protection Agency Office of Air Quality Planning and Standards, 2006). These estimates omit potential variation within a region, and may also not represent sources located outside modeled source regions well. Additionally, the impact/ton estimates generated in these studies often do not include impacts of $PM_{2.5}$ that has crossed national boundaries, which could contribute substantially to the total public health impact of a source.

In this study, we used CMAQ 4.7.1 to estimate $PM_{2.5}$-related health impacts/ton emitted for primary $PM_{2.5}$ as well as NO_x and SO_2 (through secondary $PM_{2.5}$ formation) from each of a set of power plants in one region. We then used these estimates to develop regression models that predict impacts/ton emitted for primary $PM_{2.5}$, NO_x, and SO_2, considering as predictors stack characteristics, meteorology, and the population distribution around each plant. The output of these regression models provides a method to calculate CMAQ-based impact estimates for primary $PM_{2.5}$, NO_x, and SO_2 emissions based on an individual source's emissions and location. This allows for comparison of impacts of different emitted pollutants and different sources, and the regression models can be used to estimate impacts of other emissions sources in the region. These estimates can be used in both policy and intervention design and benefit–cost analyses for interventions.

We developed this model using a set of plants within the lower Great Lakes and Mid-Atlantic region of the U.S. This region contains a large concentration of fossil energy facilities (U.S. Environmental Protection Agency, 2013), has elevated air pollution levels and a large number of at-risk individuals downwind, and is affected by current and pending state and federal regulations (Innovative Strategies and Economics Group, Office of Air Quality Planning and Standards, U.S. Environmental Protection Agency, 1999; U.S. Environmental Protection Agency Office of Air Quality Planning and Standards Health and Environmental Impacts Division, 2011; U.S. Environmental Protection Agency Office of Air and Radiation, 2011b; U.S. EPA Office of Air Quality Planning and Standards, 2009).

2. Methods

2.1. Scenario design and rationale

The two main goals of this study were to: 1) estimate the total public health impacts and impacts/ton emitted for primary $PM_{2.5}$, NO_x, and SO_2 for a set of power plants in the Mid-Atlantic and Lower Great Lakes region of the U.S., and 2) develop a regression model from these estimates predicting impacts/ton based on plant attributes, prevailing meteorology, and population distribution around each plant, allowing for application throughout the region.

A CMAQ simulation includes effects of all emission sources within its domain, but its standard implementation does not explicitly track the contributions of individual emission sources. Isolating the effects of an individual emission source using "brute force" methods would require a baseline scenario that included all sources in the domain, and a case scenario exactly the same as the baseline scenario except with the emissions from that source set to zero. Subtracting each case scenario $PM_{2.5}$ surface from the baseline $PM_{2.5}$ surface would therefore produce surfaces with $PM_{2.5}$ concentrations attributable to the zeroed source. The resulting surfaces would have concentrations of primary $PM_{2.5}$ species attributable to primary $PM_{2.5}$ emissions from the source, and concentrations of secondary $PM_{2.5}$ species attributable to SO_2 and NO_x emissions from the source. However, this alone would not allow separation of the influences of SO_2 and NO_x emissions, since SO_2 and NO_x emissions have a common influence on ambient concentrations of ammonium sulfate and nitrate. Producing separate surfaces for SO_2 and NO_x would require using two separate case scenarios, with different emissions zeroed. We applied this in our analytical design by removing both SO_2 and NO_x from one of the case scenarios, and just NO_x from the second. To determine the influence of SO_2 alone, we subtracted the influence of NO_x from the influence of both pollutants combined. The influence of a source could therefore be adequately represented using a baseline scenario and two case scenarios with differing emissions removed.

Ideally, we would have two case scenarios for every power plant in our domain, but we were constrained to 40 case runs. If we only isolated one power plant per case run, we would be restricted to 20 sources with two case scenarios per source. To include more plants in the analysis, we allowed for more than one plant to be removed in each case scenario and developed a statistical method to separate the influence of each source. To assign plants to scenarios, we first placed each of the 20 highest SO_2-emitting plants in the region in one of the 20 case scenario pairs. All emissions were removed in the first of each pair, and only NO_x and primary $PM_{2.5}$ were removed in the second of the pair. We then included between one and three additional plants in 18 of the 20 case scenario pairs. Additional plants were selected to represent the full range of plants in the region, including a variety of geographic locations, emission rates, and stack heights. Plants were assigned to case scenario pairs with as much geographic separation as possible to minimize plume overlap. To further enhance our ability to separate the contributions of each plant in a case run, we zeroed the opposite set of emissions from what was zeroed for the initial plant (if the first plant had all pollutants zeroed, the additional plants had NO_x and primary $PM_{2.5}$ zeroed, and vice versa). Within the additional plants, we included a subset of power plants with very low emissions to determine a potential threshold below which power plants could not be reasonably characterized using this scenario design and statistical separation methodology. Our final sample for the 20 case scenario pairs consisted of 51 power plants. Scenario assignments are provided in Tables S1–S2.

2.2. Method overview

With this scenario design, we implemented a 5-step analysis to estimate the public health impacts from emissions from our 51 power plants, develop estimates of impact/ton for each plant and emitted pollutant, and develop our final regression model predicting each impact/ton based on the stack characteristics, prevailing meteorology, and population distribution around each source. Each of the five sections that follow describes each step in detail, and an overview of the methodology is described below:

1. We simulated the 20 pairs of case scenarios and one baseline scenario (with no sources removed) in CMAQ (41 scenarios total), subtracting each case scenario from the baseline scenario to isolate the contribution of the selected plants' emissions;
2. We aggregated the speciated CMAQ output to primary and secondary $PM_{2.5}$ (assignments in Table S3), and visually examined the layers to determine a threshold below which low-emitting plants were likely to be undetectable using our statistical apportionment methodology;
3. We then separated the contribution of individual sources and pollutants to produce surfaces representing primary $PM_{2.5}$, secondary $PM_{2.5}$ from SO_2, and secondary $PM_{2.5}$ from NO_x emissions from each plant. For scenarios with multiple emitting plants, we implemented a statistical method to apportion $PM_{2.5}$ concentrations between emitting plants, removing plants for which the apportionment method did not meet predefined criteria;
4. We estimated the $PM_{2.5}$-related health impacts of emissions by linking U.S. and Canadian population and baseline mortality data with a literature-based concentration–response function. We calculated impacts/ton emitted for each pollutant and source, and monetized these health impacts;
5. We created a final regression model predicting impact/ton for each emitted pollutant as a function of the stack characteristics, meteorology, and population distribution around each plant.

We conducted two different diagnostic tests at different stages of the analysis (detailed below) to examine and evaluate the performance of the analytical methods, and included in our regression model-building approach a methodology to remove plants that were either poorly characterized or were influential points.

2.3. CMAQ simulations

We used 2005 emission data for SO_2, NO_2, volatile organic compounds (VOCs), carbon monoxide (CO), and $PM_{2.5}$ from the U.S. EPA National Emissions Inventory (NEI) (U.S. Environmental Protection Agency) as inputs to the CMAQ modeling framework version 4.7.1 (Byun and Ching, 1999; Byun and Schere, 2006) using Mesoscale Model 5 (MM5) version 3.7.4 (Grell et al., 1994), meteorology inputs for the year 2005 and the sparse matrix operator kernel emissions (SMOKE) version 2.7 modeling system for emission inputs (Houyoux et al., 2000). The CMAQ model domain was the 240 × 279 Eastern U.S. grid with 12 km × 12 km grid squares and simulations were run for one model year.

2.4. CMAQ output post-processing

The CMAQ output provides surfaces with concentration estimates for multiple particle constituents for each grid square, which we aggregated to produce estimates of total annual primary $PM_{2.5}$ and total secondary $PM_{2.5}$. Primary $PM_{2.5}$ was the sum of $PM_{2.5}$ elemental carbon (PM_EC), $PM_{2.5}$ as primary organic carbon (PM_POC), other primary $PM_{2.5}$ (PM_OTHER), sodium (PM_NA), chloride (PM_CL), and primarily emitted sulfate and nitrate. As there are no secondary formation pathways for PM_EC, we estimated primary sulfate and nitrate concentrations by multiplying PM_EC concentrations by the ratio of PM_EC emissions to primary sulfate and nitrate emissions. The ratio of these emissions did not vary among our sources. These primary sulfate and nitrate concentrations were subtracted from total sulfate and nitrate concentrations to calculate concentrations of secondary sulfate and nitrate. Secondary $PM_{2.5}$ is the sum of the $PM_{2.5}$ fractions of secondary sulfate (PM_SO_4), secondary nitrate (PM_NO_3), and particulate ammonium (PM_NH_3) bound to either sulfate or nitrate, and secondary organic carbon (PM_OC). Since ammonium is reported separately in CMAQ, we apportioned ammonium particle mass to secondary sulfate and nitrate using a standard post-processing methodology described elsewhere (Arunachalam et al., 2011). Briefly, we estimate particulate ammonium (PM_NH_4) bound to nitrate using the molar ratio $0.29 \times (PM\_NO_3)$, and assign the remaining particulate ammonium as being bound to sulfate. The secondary $PM_{2.5}$ represented those constituents influenced by gaseous SO_2 and NO_x emissions and related changes to atmospheric conditions. All CMAQ output was aggregated and apportioned with this approach, and the case scenario surfaces were then subtracted from the baseline scenario surface to produce "source-influence surfaces". These surfaces provided $PM_{2.5}$ concentrations attributable to all emissions removed in the case scenario. We visually inspected the $PM_{2.5}$ source-influence surfaces using scatterplots of concentration by distance from source as a first screening to determine what sources could be separated and if there was a threshold below which impacts could not be reasonably estimated given this scenario design method to separate influence of individual sources. Derivations and definitions of pollutant layers used in this analysis are given in Table S2.

2.5. Separation of individual source contributions to primary $PM_{2.5}$

Each primary $PM_{2.5}$ concentration source-influence surface represents the contribution of all primary $PM_{2.5}$ emissions from plants of interest in the corresponding case scenario. For case scenarios with more than one plant, we developed a statistical methodology to apportion the contribution of each plant and produce separate surfaces representing the contribution of primary $PM_{2.5}$ emissions from each plant.

First, we calculated the portion of total health impacts from primary $PM_{2.5}$ emissions in each case scenario pair within varying radii around the plants, to determine whether our scenario design reasonably separated impacts. We found a need to statistically separate plumes, so we used a two-step process to separate plumes. These steps are described in the following two sections in detail, and an overview is given below:

1. We approximated distance-dependent relationships from each source in these scenarios.
2. We used these distance-dependent relationships to determine the relative contribution of each source to concentrations in the source-influence surface, and use these relative contribution estimates to apportion the source-influence surface to each plant.

2.5.1. Distance-dependent relationships of $PM_{2.5}$ concentrations from each source

To develop the distance-dependent relationship, we approximated a "capture radius" for each source-influence surface as half the shortest distance between any two plants in a scenario, assuming that within this distance from each plant, elevated $PM_{2.5}$ concentrations would be largely attributable to that plant. Starting with the highest-emitting plant in the scenario, we used the grid cells within the "capture radius" of the plant to fit a distance-dependent function for primary $PM_{2.5}$ concentrations in 8 cardinal directions, using the *nls* function in R version 3.0.2 (R Core Team, 2014). The function is patterned after the

function used by Baker and Foley (2011), and replicates expected patterns of pollutant fate and transport.

$$\text{Emission contribution} = \frac{\beta_1}{1 + (\beta_2 \times \text{distance})}$$

This function, with the plant's fitted parameters, was then used to generate a surface representing the contribution of that plant to $PM_{2.5}$ throughout the source-influence surface. This statistically-derived surface was subtracted from the source-influence surface to produce a remainder surface that represents the primary $PM_{2.5}$ concentrations from all the other sources of interest in the scenario. This procedure was then repeated for the remaining plants in the scenario, in order of decreasing emissions and starting with the previous plant's remainder surface, resulting in a series of statistically-derived surfaces representing the influence of each plant of interest in the scenario.

2.5.2. Determining relative contributions of each source to the source-influence surface

We used these statistically-derived surfaces to apportion the initial source-influence surface among plants of interest represented in that surface. We created surfaces that represent the proportion of the source-influence surface that is attributable to each plant in the scenario by dividing each statistically-derived surface by the sum of all statistically-derived surfaces. Finally, we multiplied each proportion surface by the initial source-influence surface to produce a set of separate surfaces representing primary $PM_{2.5}$ concentrations from each source in the scenario.

This process statistically separates each source-influence surface into components representing the contribution of each source, while still directly linking estimates for each plant to the original surface and ensuring that the sum of the contributions of the individual plants in the run will always equal the total of the surface. While this approach clearly simplifies the complex spatially-dependent associations within CMAQ, it provides a reasonable estimate of the portion of the scenario health impacts attributable to each source.

2.6. Separation of individual source contributions of NO_x and SO_2 emissions

To produce similar surfaces for both SO_2 and NO_x for each plant, we first produced a surface representing secondary $PM_{2.5}$ from SO_2 emissions from each plant of interest by subtracting the second source-influence surface of each pair from the corresponding first source-influence surface of the pair. We then calculate the absolute value of the layer to correct for the negative concentrations produced by subtracting. To develop surfaces representing the influence of SO_2 emissions from each plant, we applied the same statistical method used for primary $PM_{2.5}$. To develop surfaces representing secondary $PM_{2.5}$ from NO_x, we subtracted the secondary $PM_{2.5}$ from SO_2 surfaces from the total secondary $PM_{2.5}$ surface. We then separate the influence of each plant in each scenario using the same statistical procedure as we did for primary $PM_{2.5}$ and SO_2, and develop separate surfaces representing secondary $PM_{2.5}$ from NO_x for each plant. This provides two NO_x surfaces for each plant — one with NO_x emitted alone, and one with NO_x co-emitted with SO_2.

2.7. $PM_{2.5}$ health impact assessment

We projected the CMAQ domain grid to USGS Lambert Conformal Conic and intersected it with 2010 U.S. Census Tracts aggregated to county level (U.S. Census Bureau) and 2011 Canadian Census Division boundaries (Statistics Canada, 2013) using R version 3.0.2 (R Core Team, 2014) and the R package *rgeos* version 0.2-17 (Bivand et al., 2014). We then calculated the population 25 years of age and over in each grid square by determining the proportion of each U.S. Census County and Canadian Census Division in each grid square, multiplying that by the population in each County or Division, and calculating total population in each grid square. This assumes that population was evenly geographically distributed throughout either the U.S. Census county or Canadian Census Division. Mortality rates within each grid square were then calculated using population-weighted average U.S. county-level mortality rates for 1999–2010 from the U.S. Centers for Disease Control and Prevention WONDER database (U.S. Centers for Disease Control and Prevention, National Center for Health Statistics, 2013) and average Canadian Division-level mortality rates for 1999–2010 (Statistics Canada, 2013).

The mortality attributable to each plant's emissions was then calculated by merging the population data, baseline mortality rate, the annual $PM_{2.5}$ concentration surfaces for each emitted pollutant from each plant, and a concentration–response function of a 1.06% increase in mortality risk per 1 $\mu g/m^3$ increase in annual average $PM_{2.5}$ concentration (Roman et al., 2008; Schwartz et al., 2008; U.S. Environmental Protection Agency Office of Air and Radiation, 2010, 2011b). The excess mortality cases were then monetized using the value of statistical life, an estimate of the societal value of a small reduction in mortality risk. We applied a value of $7.2 million (2010 USD), commonly used in U.S. EPA regulatory impact analyses, health risk assessments, and other applications (Dockins et al., 2004; Levy et al., 2009; Muller et al., 2011; National Research Council, 2010). This produced estimates of attributable mortality for each emitted pollutant from each power plant in terms of both number of cases and monetized health impact cost. Since the estimates of total impact for each pollutant contain impacts from all plants in the initial CMAQ scenario, not just those that could be detected using our apportionment algorithm and are therefore in our final sample, we developed our impact/ton estimate by apportioning the emissions of undetectable plants between the detectable plants. We used the mean of the two NO_x estimates for each plant as our final NO_x impact/ton estimate. For scenarios with only one discernible plant, we were able to generate estimates of impacts/ton emitted for each particle species (i.e., separate estimates for ammonium nitrate/ton of NO_x emitted and ammonium sulfate/ton of NO_x emitted).

In addition to the diagnostic tests during the analysis, we also examined the distribution of impact per ton estimates for significant outliers, inspecting values to determine if the value depended on the emission rate, fit of the apportionment algorithm, or other factors not causally related to the magnitude of damages. At this stage, we removed from the primary $PM_{2.5}$ analysis any plants where the curve-fitting algorithm failed to discern any influence from the emissions, defined as a value of zero for β_1 coefficient in the curve-fitting in any direction, and removed from both the SO_2 and the NO_x analysis any plant that failed either SO_2 or NO_x.

2.8. Construction of final regression model

We constructed a linear regression model to explain the plant-to-plant variability in impacts/ton for primary $PM_{2.5}$, SO_2, and NO_x, using physically interpretable predictors and functional form. We therefore focused on population terms within various annuli in the east (downwind) and west (upwind) directions, with no intercept included to reflect the fact that impacts would be zero if exposed population were zero. We also tested interaction terms between stack height and population. We selected distances for the annuli that maximized predictive power with a small number of covariates. Preliminary model-building indicated that three population terms were most predictive across models — population within 100 km (in all directions), 100–500 km east, and 500–2000 km east of each plant.

To make models for each pollutant that could be applied to sources across the region in other studies, but still maintain physical interpretability, we followed a model-building procedure starting with a no-intercept model and the three population terms. We then removed the least significant variable and reran this next model until only significant variables remained. We then tested this candidate model for

influential points using a Cook's Distance test, and removed points with Cook's Distance greater than 4/(degrees of freedom) (Cook and Weisberg, 1982). As an additional QA/QC measure, we then manually examined the statistically-derived pollutant layers for all highly influential plants that remained, along with pollutant layers for a sample of the less influential plants. We removed any plants with pollutant layers that exhibited features that were more likely due to the apportionment algorithm, such as serious deviations from the expected exponential decay with distance or extremely sharp changes in pollutant concentrations. With this trimmed sample of power plants, we retested the candidate model and versions of the model including an intercept and previously removed variables, and removed least significant predictors until we had a new candidate model with only significant predictors. We then performed the Cook's Distance diagnostic again, and similar retesting on the model until we produced a final model. To test the validity and generalizability of these final models, we performed a 5-fold cross-validation procedure using these final model variables. This method randomly splits each data set into 5 groups or "folds". Four folds are used as a model training set and one is used as a verification set — a regression model is derived from this training set using the same variables as our main regression, and the results of this regression model are used to predict impacts/ton for the verification set. This method is then repeated with each fold serving as the verification set.

3. Results

3.1. Performance and diagnostics

The 40 CMAQ scenarios included a total of 51 plants. However, initial examination of CMAQ outputs and application of the methods to separate emission contributions suggested that the influence of many low-emitting plants could not be separated from higher-emitting plants. Therefore, we removed plants that emitted less than 10 tons of primary $PM_{2.5}$, 1000 tons of SO_2, or 500 tons of NO_x per year, leaving 38 plants for our analyses. After removing plants that could not be separated with the apportionment algorithm, we were left with 35 impact/ton estimates for primary $PM_{2.5}$, and 20 for both SO_2 and NO_x that were used to construct the final regression model. For primary $PM_{2.5}$, three plants were over the Cook's Distance threshold, and an additional 5 plants were removed after manual examination, leaving 27 plants in the final primary $PM_{2.5}$ model. For SO_2, two plants were over the Cook's Distance threshold and one additional plant was removed after the manual examination, leaving 17 plants in the final SO_2 model. For NO_x, one plant was over the Cook's Distance threshold, and three plants were removed after the manual examination, leaving 16 plants in the NO_x final models. Results from the plants in these final models are displayed here.

The apportionment algorithm was able to separate the influence of the final set of plants reasonably well with generally well-defined distance-dependent relationships. Across the final power plants and wind directions, the r^2s for primary $PM_{2.5}$ had a median of 0.999 (range 0.992–0.999); for SO_2, a median of 0.999 (range 0.994–0.999); and for both NO_x estimates, a median of 0.996 (range 0.977–0.999). Secondary $PM_{2.5}$ formation from SO_2 emissions follows an exponential decay with distance, and examination of particle constituents shows the anticipated "nitrate bounce-back", where SO_2 emissions react with free ammonium and suppress formation of nitrates and a very small contribution from induced organic carbon aerosol formation (Figs. S3, S11, S15). Secondary $PM_{2.5}$ formation from NO_x emissions follows a more variable pattern as a function of distance, largely due to different formation patterns of sulfate, nitrate, and organic carbon aerosols (Figs. S1–S4). Nitrate formation from NO_x exhibits a complex and occasionally non-monotonic association with distance, as anticipated given the complexities of sulfate–nitrate–ammonium reactions. Secondary $PM_{2.5}$ from NO_x consisted of an appreciable portion of sulfate, and a very small portion of organic carbon aerosols, both of which followed an exponential decay with distance (Figs. S5–S10, S12, S14, S16).

There were 8 scenarios that either had one plant or had two plants, one of which was below our initial emission cutoff. We used these runs to determine the proportionate contribution of the different constituents of the secondarily formed $PM_{2.5}$ to the total impacts of SO_2 and NO_x emissions. For SO_2, ammonium sulfate contributed a median of 112% (range: 105%–116%), ammonium nitrate contributed a median of −13% (range: −5% to −16%), and organic carbon aerosols contributed a median of 0.4% (range: 0.2%–0.5%). For NO_x emissions, ammonium sulfate contributed a median of 66% of the impact (range: 25%–79%), ammonium nitrate contributed a median of 34% of the impact (range: 20%–75%), and organic carbon contributed a median of 0.7% (range: −0.2%–1.4%) (Fig. 1). All percentages are by mass.

When the apportionment algorithm was used to estimate impacts/ton, there was more variability for low-emitting plants than for high-emitting plants, which could either be explained by more variability in plant characteristics or greater error for lower emitters. Examining the associations of impact per ton as a function of emissions, there appear to be limited biases but increased errors for low-primary $PM_{2.5}$-emitting plants, increased errors and potentially underestimated impacts for low-SO_2-emitting plants, and increased errors and potentially overestimated impacts for low-NO_x-emitting plants.

3.2. Impact estimates, predictors, regression results, and cross-validation

Plants included in our final analysis had a median health impact estimate of $130,000/ton for primary $PM_{2.5}$ (range: $22,000–230,000), $28,000/ton for secondary $PM_{2.5}$ attributable to SO_2 emissions (range: $19,000–33,000), and $16,000/ton for secondary $PM_{2.5}$ attributable to NO_x emissions (range: $7100–26,000) (Fig. 2). Impacts occurring in Southern Canada contributed to the total impact/ton a median of 2.9% (range: 0%–6.8%) for primary $PM_{2.5}$, 5.4% (range: 0.6%–7.2%) for secondary $PM_{2.5}$ attributable to SO_2 emissions, and 6.1% (range: 0.37%–11.3%) for secondary $PM_{2.5}$ attributable to NO_x emissions. Plants with the highest impacts/ton of primary $PM_{2.5}$ tend to be near and immediately upwind of major population centers. Plants with high impacts/ton of SO_2 and NO_x tended to be slightly further upwind of major population centers, with more variability for NO_x (Graphical Abstract).

At least one population variable significantly predicted impacts/ton for each pollutant (Table 1). Population within 100 km and population 100–500 km east of the source were a significant predictor for primary $PM_{2.5}$ impacts/ton emitted. All three population variables were significant for SO_2 impacts/ton emitted, and just population 100–500 km was significant for NO_x impacts/ton emitted. The regression parameter estimates for primary $PM_{2.5}$ and SO_2 decrease with distance (Table 1). Our regression models explained 88–99% of variability in impact/ton estimates across the three emitted pollutants, albeit in zero intercept models (Table 1). Use of stack height as an interaction term was not statistically significant for any emitted pollutant.

The training regressions in the 5-fold cross-validation were able to explain between 87 and 99% of variation in impacts/ton, with stable regression coefficients and relatively small errors in predicted values. The predictions from the training regressions had a median percent error of −9.7% (IQR: −32% to 19%) for primary $PM_{2.5}$, −0.2% (IQR: −4.8% to 4.1%) for SO_2, and −10.7% (IQR: −20% to 20%) for NO_x (Fig. S17).

4. Discussion

Our modeling approach provided distributions of the $PM_{2.5}$-related health impacts/ton of emissions for individual power plants simulated using CMAQ, which allowed us to include the complexities of secondary particulate matter formation in examining between-plant variability.

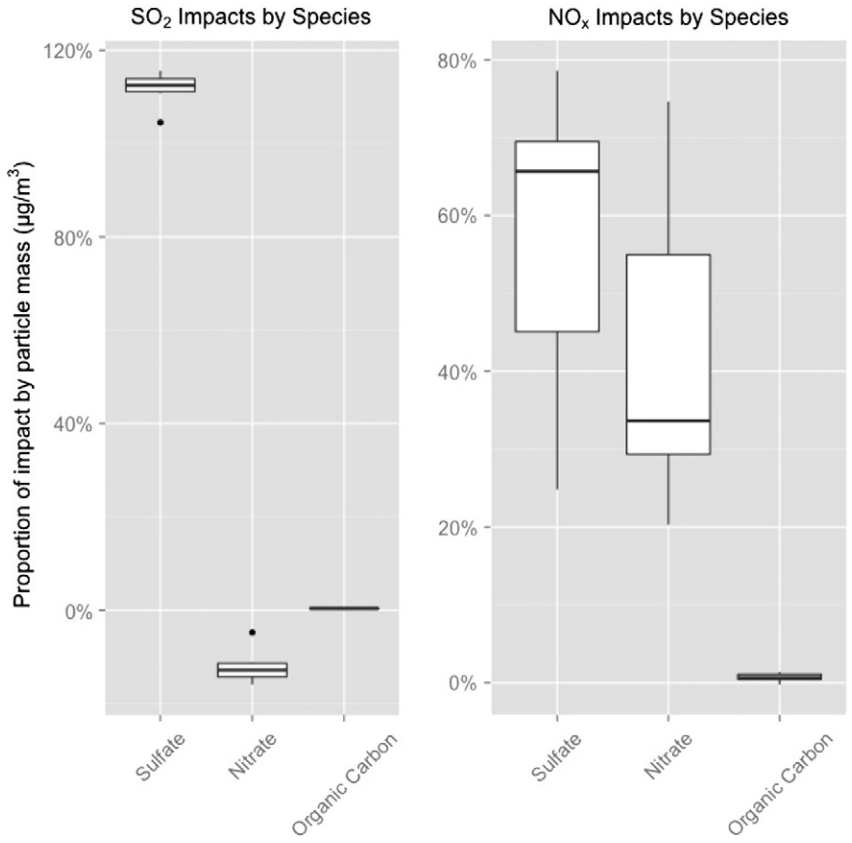

Fig. 1. Impacts of emissions of SO_2 and NO_x by secondary $PM_{2.5}$ species type for a subset of 8 runs with one plant as the main emission source.

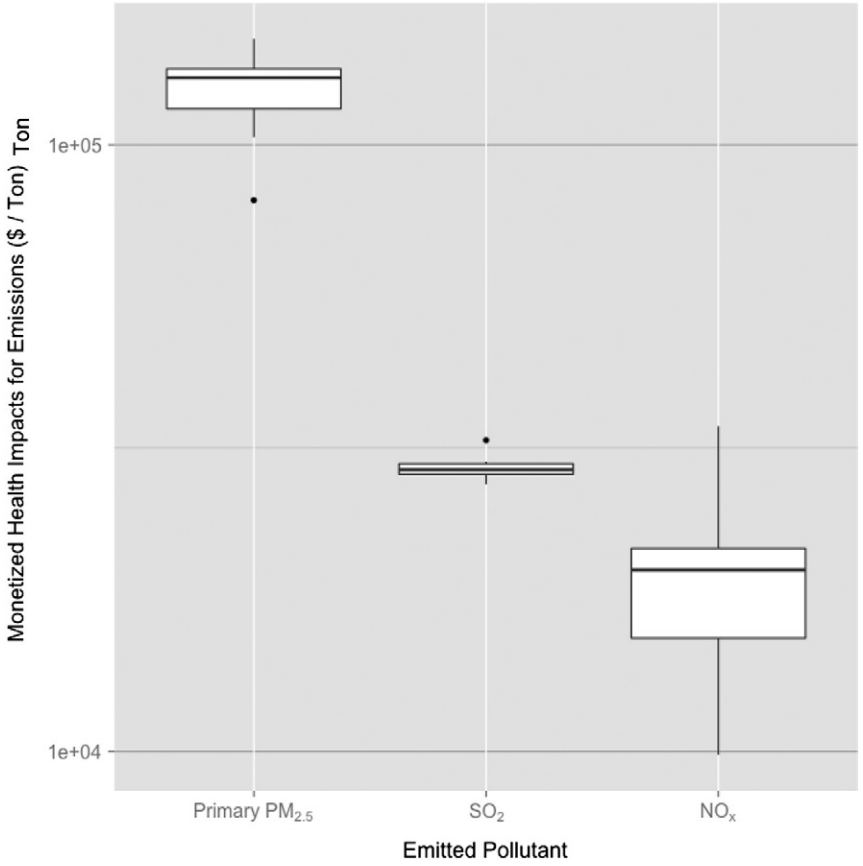

Fig. 2. Monetized estimates of PM-related public health impacts/ton occurring in both the United States and Canada for emissions from a set of power plants, by emission type. Influential points, determined by Cook's Distance, and plants where the apportionment algorithm did not pass manual diagnostics, were removed.

Table 1
Regression models predicting monetized $PM_{2.5}$-related public health impacts ($/ton emitted) as a function of population distribution around each power plant.

	Estimate	Std. error	t value	Pr(>|t|)
Primary $PM_{2.5}$				
Population 0–100 km	1.09E−02	4.00E−03	2.74	1.11E−02
Population 100–500 km East	4.11E−03	5.07E−04	8.11	1.84E−08
Adjusted $r^2 = 0.88$, n = 27				
SO_2				
Population 0–100 km	2.11E−03	5.98E−04	3.52	3.38E−03
Population 100–500 km East	6.26E−04	7.10E−05	8.81	4.36E−07
Population 500–2000 km East	1.59E−04	2.15E−05	7.38	3.46E−06
Adjusted $r^2 = 0.99$, n = 17				
NO_x				
Population 100–500 km East	6.86E−04	4.46E−05	15.4	1.37E−10
Adjusted $r^2 = 0.94$ n = 16				

The monetized impact/ton estimates for primary $PM_{2.5}$ and SO_2 are near the values of previous analyses that used simplified chemistry and transport models and the same concentration–response function for $PM_{2.5}$ used here (Levy et al., 2009; U.S. Environmental Protection Agency Office of Air and Radiation, 2010), and were comparable to other studies after adjusting for different concentration–response functions and other key parameters (Muller and Mendelsohn, 2007; Muller et al., 2011; National Research Council, 2010). The training regressions developed during cross-validation could all explain over 88% of the variability in impacts/ton, and the median and interquartile range of the percent errors were relatively close to zero, although with extreme values for a few plants (Fig. S17). This provides reassurance both that simpler models could adequately capture total population exposure to $PM_{2.5}$ concentrations from primary $PM_{2.5}$ and SO_2 emissions and that our CMAQ modeling and apportionment approach yielded interpretable values for impacts/ton emitted.

Additionally, since our scenario design removes emissions from one source or a few sources spread out over a large geographical region, we do not substantially alter background chemistry; this ensures that our scenario design represents individual source effects, and not effects due to changes in background chemistry. Our SO_2 impact/ton estimates could theoretically be affected by changes in plume chemistry since our SO_2 estimates are based in part on simulations where both SO_2 and NO_x are removed. To test this, we calculated the ratio of SO_2 and NO_x emissions for each source used to develop our final SO_2 impact/ton estimates, and performed a linear regression to test the relationship between the SO_2/NO_x emissions ratio and our SO_2 impact/ton estimates. This relationship was not statistically significant ($p = 0.55$), which indicates that co-emissions of NO_x are not a major influence on SO_2 impact/ton values. More generally, the SO_2 impact/ton values fell into a fairly narrow range ($19,000–33,000) across power plants with widely varying ratios between SO_2 and NO_x emissions, the estimates were similar to those found previously in the literature, and the population-based regression had good statistical properties, so we are confident that we have developed robust estimates for the $PM_{2.5}$-related health impacts/ton of SO_2 emissions.

However, our estimates for the $PM_{2.5}$-related health impacts/ton of NO_x emissions are higher than what many previous analyses found (Fann et al., 2012a, 2012b; Levy et al., 2009; National Research Council, 2010). This is likely due to complexities of NO_x chemistry present in CMAQ 4.7.1, but not present in simpler models. Beyond interactions with background ammonium to form ammonium nitrate, NO_x emissions are also involved in the ozone production cycle, and since ozone interacts with SO_2 and VOCs to form ammonium sulfate and secondary organic carbon particles, increasing ozone concentrations can amplify production of these particles (Byun and Schere, 2006; Saltzman et al., 1983; Stein and Saylor, 2012; U.S. Environmental Protection Agency Office of Air Quality Planning and Standards, 1999). Sulfate is formed through reactions of SO_2 with OH radicals in the atmosphere. Emissions of NO_x amplify the formation of ozone, and therefore act to increase the concentration of OH radicals in the atmosphere. This increase in the concentration of OH radicals acts to accelerate the transformation of SO_2 to sulfate particles. The model results exhibit this phenomenon largely during ozone season (Figs. S13–14), which is consistent with this formation pathway. Details of these chemical reaction mechanisms are available in the Supplemental material.

Most prior atmospheric fate and transport models used to derive damage functions, especially simplified ones, neglect these formation pathways (Greco et al., 2007; Innovative Strategies and Economics Group, Office of Air Quality Planning and Standards, U.S. Environmental Protection Agency, 1999; Levy et al., 2009; U.S. Environmental Protection Agency, 1999). CMAQ v4.7.1 contains many updates to chemical mechanisms that are relevant to this chemical pathway, and can alter the sensitivity of the formation of ammonium nitrate and ammonium sulfate to emissions of NO_x and SO_2. A major update was a new gas-phase chemistry mechanism that provides better predictions of ozone concentrations, particularly over urban areas. This update affected much of the chemistry of how NO_x affects the ozone cycle and the formation of ozone and the OH radicals, which are also involved in the formation of sulfate. There were also updates to ISORROPIA, the CMAQ module that handles thermodynamic equilibrium of inorganic aerosols. Notably, many of these updates have occurred since CMAQ v4.4, which was used in one study to estimate impacts of emission reductions of NO_x and SO_2 (Fann et al., 2009). Our analyses indicate that omitting the ability of NO_x emissions to amplify sulfate formation through the oxidation pathway now present in CMAQ 4.7.1 would lead to a systematic underestimation of impacts/ton of NO_x emitted, potentially by a factor of 3, given our finding that ammonium sulfate contributes approximately 2/3 of the total impact of NO_x emissions. This effect does appear to be present both in the presence and absence of co-emitted SO_2, since the impact/ton values for NO_x emitted alone and emitted in the presence of SO_2 are similar and reasonably correlated (Pearson correlation coefficient = 0.54, with nearly all estimates falling close to the 1:1 line) (Fig. S18), although simulations running NO_x alone, SO_2 alone, and both together would be required to better characterize effects of individual emissions and possible interactions between emitted pollutants.

We were also able to explain most variability in the impact/ton estimates using basic population covariates. In spite of the simplicity of the functional form, the regression results exhibit behavior that is consistent with regional meteorology, population distributions, and known physical and chemical behavior of these emissions. The population coefficients for primary $PM_{2.5}$ decrease with distance and are not statistically significant at distances over 500 km, consistent with expected behavior. Population coefficients for secondary $PM_{2.5}$ from SO_2 also decrease with distance but are more significant at longer range, likely reflecting time for the necessary reactions to occur. A similar pattern of multiple population predictors with monotonically decreasing coefficients was not found in the model of secondary $PM_{2.5}$ from NO_x, but this is not unexpected given the challenge of explaining complex non-linear patterns with simple regression terms. However, even in this case, the regression model demonstrated the ability to reasonably estimate impacts/ton emitted, and by extension, total impacts for other plants in the same geographic domain.

Beyond the core findings, another key aspect of our study was the analytical approach, in which we chose to simulate impacts of multiple power plants in each scenario and then statistically separate impacts of each plant, potentially increasing the sample size with which to explore variability in impact/ton estimates but potentially increasing uncertainty in these as well. For primary $PM_{2.5}$, the run design and curve-fitting algorithm performed reasonably well at separating the influence of individual plants in each CMAQ layer, except for low-emitting sources. There was increased variability in impact/ton estimates for low emitting plants, potentially reflecting errors in the curve-fitting process. Both our inability to detect very low-emitting sources and the higher variability

for low-emitting plants are likely due to the inability of the apportionment algorithm to detect the influence of the low-emitting sources over the influence of the high-emitting plants it shared runs with and, not a weakness of CMAQ or other photochemical models.

This methodology did not perform as well separating individual source contributions to secondary $PM_{2.5}$ from SO_2 and NO_x. The greater spatial extent of secondary $PM_{2.5}$ from SO_2, coupled with the involvement of atmospheric chemistry, may in part explain the greater error in characterizing long-range impacts, with a corresponding influence on apportionment of impacts across plants. Model performance was somewhat poorer for secondary $PM_{2.5}$ from NO_x, which is unsurprising given its complex chemistry, which makes the creation of a simple mathematical model difficult. A portion of the uncertainty in estimating secondary $PM_{2.5}$ from NO_x emissions may also be due to general analytical design, since in many cases accurate estimation of NO_x impacts was dependent on estimates of the influence of SO_2 emissions. This uncertainty is somewhat limited by the fact that only plants with discernable influence from both SO_2 and NO_x were included in either the SO_2 and NO_x analyses. Our design was based in part on the assumption that NO_x emissions would have a limited influence on sulfate concentrations, enhancing separability, but this assumption proved to be incorrect due to the finding of substantial ammonium sulfate formation induced by NO_x emissions. More generally, our stepwise diagnostic tests led to the removal of a large number of power plants from the analysis, which begs the question of the utility of our approach over CMAQ runs with individual plants. However, simply modeling 20 individual power plants would not have allowed us to evaluate emission thresholds or relative differences in emissions between sources where impacts could not be reasonably estimated with this simulation design and separation methodology, and our analytical approach may have value in multiple future investigations. Similar to the case with primary $PM_{2.5}$, our inability to detect low-emitting plants, and the higher variability in impact/ton estimates for low-emitting plants are likely a weakness of our simulation design and the apportionment algorithm, not a weakness of CMAQ or other photochemical models. Broadly, approaches such as CMAQ DDM have significant advantages over brute-force modeling with statistical extrapolation given some of the issues above. That said, it will remain computationally challenging to model all individual sources directly even with CMAQ DDM, and there will be value in statistical approaches to extrapolate damage function estimates for the foreseeable future, especially since parts of this methodology could be used in conjunction with CMAQ DDM. Moreover, our focus on aggregate damage/ton estimates decreases the uncertainties associated with statistical extrapolation approaches.

Beyond issues with assigning CMAQ outputs to individual plants, a few additional limitations should be acknowledged. There is some residual variability in the impact/ton estimates for these plants that is not explained by our simplified regressions. However, there are no apparent geographical patterns in the residuals that would indicate systematic errors related to meteorology or atmospheric chemistry, and the errors are generally low for most plants. These values are normalized to impacts/ton, so they can be used with present-day emissions to calculate present-day impacts, despite decreases in total emissions since 2005. However, these impact/ton estimates may still not be completely representative of present day, since they are dependent on background chemistry and meteorology, which have changed and will continue to change due to factors including continuing decreases in SO_2 emissions in the Clean Air Act (U.S. Environmental Protection Agency Office of Air Quality Planning and Standards, 2006), other policies influencing emissions from electricity and other sources (U.S. Environmental Protection Agency Office of Air Quality Planning and Standards Health and Environmental Impacts Division, 2011; U.S. Environmental Protection Agency Office of Air and Radiation, 2011a), and climate change (The Interagency Working Group on Climate Change and Health, 2010). Studies have shown that evolving background concentrations could increase the secondary $PM_{2.5}$ impact per unit NO_x emissions, and in some settings, per unit SO_2 emissions as well (Levy et al., 2012). We also focus exclusively on $PM_{2.5}$-related mortality, which will underestimate damages for all emitted pollutants by omitting $PM_{2.5}$-related morbidity and will systematically underestimate the impact/ton of NO_x emissions by omitting ozone-related impacts.

In spite of these limitations, our analysis makes some important contributions. We were able to obtain reliable estimates of impacts/ton of emissions for individual power plants based on CMAQ results. Use of this more complex atmospheric chemistry and transport model allowed us to capture the complex chemical pathways for secondary $PM_{2.5}$ formation, and include public health impacts occurring at long range from sources. Our approach led to significantly greater impacts/ton of NO_x emissions than previously estimated, since we included sulfate formation through amplified oxidation. Even with the complex chemistry, our regression modeling approach and cross-validation showed that impacts/ton can be reasonably predicted from the population distribution downwind of each power plant. While these aggregated impact/ton metrics omit spatial details important for many applications, they can be used to compare impacts of different emitted pollutants and different sources, and the monetized metrics are useful in benefit–cost analyses and to inform the design of interventions.

Funding sources

This work was supported by a grant from the Heinz Endowments (grant number C2988), the Charles F. Wilinsky award at Harvard School of Public Health, and funds from the Mark and Catherine Winkler Foundation.

Conflict of interest

The authors declare no competing financial interests.

Appendix A. Supplementary data

Supplementary data to this article can be found online at http://dx.doi.org/10.1016/j.envint.2014.03.031.

References

Arunachalam S, Wang B, Davis N, Baek BH, Levy JI. Effect of chemistry-transport model scale and resolution on population exposure to $PM_{2.5}$ from aircraft emissions during landing and takeoff. Atmos Environ 2011;45(19):3294–300. [Jun].

Baker KR, Foley KM. A nonlinear regression model estimating single source concentrations of primary and secondarily formed $PM_{2.5}$. Atmospheric Environment, 45(22). Elsevier Ltd.; 2011. p. 3758–67. [Jul 1].

Bergin MS, Russell AG, Odman MT, Cohan DS, Chameides WL. Single-source impact analysis using three-dimensional air quality models. Journal of the Air & Waste Management Association, 58(10). Taylor & Francis; 2008. p. 1351–9.

Bivand R, Rundel C, Pebesma E, Hufthammer KO KO. rgeos [Internet]. 0 ed. Available from http://cran.r-project.org/web/packages/rgeos/index.html, 2014.

Byun D, Schere K. Review of the governing equations, computational algorithms, and other components of the models-3 Community Multiscale Air Quality (CMAQ) modeling system. Appl Mech Rev 2006;59:51.

Byun DW, Ching J. Science algorithms of the EPA models-3 community multiscale air quality (CMAQ) modeling system. Washington, DC, USA: US Environmental Protection Agency, Office of Research and Development; 1999.

Cook RD, Weisberg S. Residuals and influence in regression. New York: Chapman and Hall; 1982.

Dockins C, Maguire K, Simon N, Sullivan M. Value of statistical life analysis and environmental policy: a white paper. US Environmental Protection Agency National Center for Environmental Economics; 2004.

Epstein PR, Buonocore JJ, Eckerle K, Hendryx MS, Stout Iii BM, Heinberg R, et al. Full cost accounting for the life cycle of coal. Ann N Y Acad Sci 2011;1219:73–98. [Feb].

Fann N, Baker KR, Fulcher CM. Characterizing the $PM_{2.5}$-related health benefits of emission reductions for 17 industrial, area and mobile emission sectors across the U.S. Environ Int 2012 Novb;49:141–51.

Fann N, Fulcher CM, Baker K. The recent and future health burden of air pollution apportioned across U.S. sectors. Environ Sci Technol 2013;47(8):3580–9. [Apr 16].

Fann N, Fulcher CM, Hubbell BJ. The influence of location, source, and emission type in estimates of the human health benefits of reducing a ton of air pollution. Air Qual Atmos Health 2009;2(3):169–76. [Sep].

Fann N, Lamson AD, Anenberg SC, Wesson K, Risley D, Hubbell BJ. Estimating the national public health burden associated with exposure to ambient $PM_{2.5}$ and ozone. Risk Anal 2012a;32(1):81–95. [Jan].
Greco SL, Wilson AM, Spengler JD, Levy JI. Spatial patterns of mobile source particulate matter emissions-to-exposure relationships across the United States. Atmospheric Environment, 41(5). Elsevier; 2007. p. 1011–25.
Grell GA, Dudhia J, Stauffer DR. A description of the fifth-generation Penn State/NCAR mesoscale model (MM5); 1994.
Houyoux MR, Vukovich JM, Coats Jr CJ, Wheeler NJM, Kasibhatla PS. Emission inventory development and processing for the Seasonal Model for Regional Air Quality (SMRAQ) project. J Geophys Res 2000;105(D7):9079. [Apr 1].
Innovative Strategies and Economics Group, Office of Air Quality Planning and Standards, U.S. Environmental Protection Agency. Regulatory impact analyses for the particulate matter and ozone National Ambient Air Quality Standards and proposed regional haze rule. NC: Research Triangle Park; 1999 [Jul].
Itahashi S, Uno I, Kim S. Source contributions of sulfate aerosol over East Asia estimated by CMAQ-DDM. Environ Sci Technol 2012;46(12):6733–41. [Jun 19].
Levy J, Spengler J. Modeling the benefits of power plant emission controls in Massachusetts. J Air Waste Manage Assoc 2002;52(1):5–18.
Levy J, Spengler J, Hlinka D, Sullivan D, Moon D. Using CALPUFF to evaluate the impacts of power plant emissions in Illinois: model sensitivity and implications. Atmos Environ 2002;36(6):1063–75.
Levy J, Wilson A, Evans J, Spengler J. Estimation of primary and secondary particulate matter intake fractions for power plants in Georgia. Environ Sci Technol 2003; 37(24):5528.
Levy JI, Baxter LK, Schwartz J. Uncertainty and variability in health-related damages from coal-fired power plants in the United States. Risk Anal 2009;29(7):1000–14. [Jul 1].
Levy JI, Woody M, Baek BH, Shankar U, Arunachalam S. Current and future particulate-matter-related mortality risks in the United States from aviation emissions during landing and takeoff. Risk Anal 2012;32(2):237–49. [Feb].
Machol B, Rizk S. Economic value of U.S. fossil fuel electricity health impacts. Environ Int 2013;52:75–80. [Feb].
Muller N, Mendelsohn R. Measuring the damages of air pollution in the United States. J Environ Econ Manage 2007;54(1):1–14.
Muller NZ, Mendelsohn R. Efficient pollution regulation: getting the prices right. AmericanEconomic Review, 99(5). American Economic Association; 2009. p. 1714–39. [Dec].
Muller NZ, Mendelsohn R, Nordhaus W. Environmental accounting for pollution in the United States economy. Am Econ Rev 2011;101(5):1649–75. [Aug].
National Research Council. Hidden costs of energy: unpriced consequences of energy production and use; 2010.
Pope III C, Burnett R, Thun M, Calle E, Krewski D, Ito K, et al. Lung cancer, cardiopulmonary mortality, and long-term exposure to fine particulate air pollution. JAMA 2002; 287(9):1132.
Pope CA, Dockery DW. Health effects of fine particulate air pollution: lines that connect. J Air Waste Manag Assoc 2006;56(6):709–42. [Jun 1].
R Core Team. A language and environment for statistical computing [Internet]. R Foundation for Statistical Computing2nd ed. . Ustria: Vienna; 2014. Available from: http://www.R-project.org/.
Roman H, Walker K, Walsh T, Conner L, Richmond H, Hubbell B, et al. Expert judgment assessment of the mortality impact of changes in ambient fine particulate matter in the US. Environ Sci Technol 2008;42(7):2268–74.
Saltzman ES, Brass GW, Price DA. The mechanism of sulfate aerosol formation: chemical and sulfur isotopic evidence. Geophys Res Lett 1983;10(7):513.
Schwartz J, Coull B, Laden F, Ryan L. The effect of dose and timing of dose on the association between airborne particles and survival. Environ Health Perspect 2008; 116(1):64.
Statistics Canada. Boundary Files [Internet]. Statistics Canada. Available from: http://www12.statcan.gc.ca/census-recensement/2011/geo/bound-limit/bound-limit-eng.cfm, 2013.
Statistics Canada. CANSIM Table 051–0053. Statistics Canada 2013.
Stein AF, Saylor RD. Sensitivities of sulfate aerosol formation and oxidation pathways on the chemical mechanism employed in simulations. Atmos Chem Phys 2012;12:8567–74.
The Interagency Working Group on Climate Change. A human health perspective on climate change; 2010. p. 1–80 [Apr 20].
U.S. Census Bureau. 2010 Census TIGER/Line Shapefiles Pre-Joined with 2010 Census Demographic Profile [Internet]. Available from: http://www.census.gov/geo/www/tiger/tgrshp2010/2010DP1.html, 2010.
U.S. Centers for Disease Control and Prevention, National Center for Health Statistics. CDC WONDER [Internet]. U.S. CDC. Available from: http://wonder.cdc.gov/cmf-icd10.html, 2013.
U.S. Environmental Protection Agency. Regulatory impact analysis — control of air pollution from new motor vehicles: tier 2 motor vehicle emissions standards and gasoline sulfur control requirements. lobby.la.psu.edu, 1999. [Dec].
U.S. Environmental Protection Agency. Emissions & generation resource integrated database [Internet] 2007 ed. U.S. Environmental Protection Agency; 2013 [Available from: http://www.epa.gov/cleanenergy/energy-resources/egrid/index.html].
U.S. Environmental Protection Agency. National Emissions Inventory [Internet]. Available from: http://www.epa.gov/ttn/chief/net/2005inventory.html#inventorydata.
U.S. Environmental Protection Agency Office of Air and Radiation. Quantitative health risk assessment for particulate matter [Internet] ; 2010 [epa.gov. [cited 2012 Nov 7]. Available from: http://www.epa.gov/ttn/naaqs/standards/pm/data/PM_RA_FINAL_June_2010.pdf].
U.S. Environmental Protection Agency Office of Air and Radiation. Regulatory impact analysis for the federal implementation plans to reduce interstate transport of fine particulate matter and ozone in 27 states; correction of SIP approvals for 22 states. epa.gov, 2011. [Jun].
U.S. Environmental Protection Agency Office of Air and Radiation. The benefits and costs of the Clean Air Act from 1990 to 2020; 2011b. p. 1–238 [Feb].
U.S. Environmental Protection Agency Office of Air Quality Planning and Standards. Nitrogen oxides (NO_x) why and how they are controlled. books.google.com, 1999.
U.S. Environmental Protection Agency Office of Air Quality Planning and Standards. Technical support document for the proposed PM NAAQS rule. epa.gov, 2006. [Feb].
U.S. Environmental Protection Agency Office of Air Quality Planning and Standards Health and Environmental Impacts Division. Regulatory impact analysis for the final mercury and air toxics standards. epa.gov, 2011. [Dec].
U.S. EPA Office of Air Quality Planning and Standards. Technical support document for the final clean air interstate rule [Internet] 2009; 2009 [Mar. Available from: http://www.epa.gov/cair/pdfs/finaltech02.pdf].
Weber C, Jaramillo P, Marriott J, Samaras C. Life cycle assessment and grid electricity: what do we know and what can we know? Environ Sci Technol 2010;44(6): 1895–901.
Zanobetti A, Schwartz J. The effect of fine and coarse particulate air pollution on mortality: a national analysis. Environ Health Perspect 2009;117(6):898–903. [Jun 1].